

tinguishable with respect to the polarization properties from the case when the echo is formed in two independent transitions, each of which belongs to the  $Q$  branch. A similar remark holds also for the second group of transitions and for the case of formation of an echo on two independent transitions, each of which belongs to the  $P(R)$  branch, or one of them belongs to the  $P$  branch and the other to the  $R$  branch.

The line 5 in the figure is a plot of  $\theta_e$  against  $\psi$  when the echo is formed on two independent transitions, one of which belongs to the  $Q$  branch and the other to the  $P$  or  $R$  branch. This polarization dependence is obtained from Ref. 5 if the echo is formed on two independent transitions:  $j_1 \rightarrow j_1(j_1 \gg 1)$  and  $j_2 \rightarrow j_2 + 1(j_2 \gg 1)$  at  $N_{01} = N_{02}$ ,  $|d_1| = |d_2|$  and  $(\omega_{01} - \omega_{02})\tau_s \ll 1$ . Here  $N_0$ ,  $d_1$ , and  $\omega_{01}$  are the density of the excess population, the reduced dipole moment, and the frequency for the  $j_1 \rightarrow j_1$  transition, while  $N_{02}$ ,  $d_2$ , and  $\omega_{02}$  are the analogous quantities for the transition  $j_2 \rightarrow j_2 + 1$ .

We note that the comparison of the experimental curves with those of the figure should be made at small areas of the exciting pulses, when the theory considered here is valid. This points for the need of organizing new experiments aimed at identifying molecular transitions by the photon-echo method.

We note in conclusion that if  $\tau_s$  is comparable with the times of the irreversible relaxation, then the intensity of the echo will attenuate with time in accord with an exponential law that takes at  $\gamma_{ab} = \gamma_{ab}$  the form  $\exp(-2\gamma_{ab}t)$ .

The authors thank A. I. Alekseev, S. S. Alimpiev, and

N. V. Karlov for a discussion of the results.

- <sup>1</sup>A. I. Alekseev and I. V. Evseev, Zh. Eksp. Teor. Fiz. **56**, 2118 (1969); **57**, 1735 (1969) [Sov. Phys. JETP **29**, 1139 (1969); **30**, 938 (1970)].
- <sup>2</sup>J. P. Gordon, C. H. Wang, C. K. N. Patel, R. E. Slusher, and W. J. Tomlinson, Phys. Rev. **179**, 294 (1969).
- <sup>3</sup>V. Heer and R. H. Kohl, Phys. Rev. A **1**, 693 (1970); **2**, 549 (1970).
- <sup>4</sup>C. V. Heer and R. J. Nordstrom, Phys. Rev. A **11**, 536 (1975).
- <sup>5</sup>I. V. Evseev and V. M. Ermachenko, Zh. Eksp. Teor. Fiz. **76**, 1538 (1979) [Sov. Phys. JETP **49**, 780 (1979)].
- <sup>6</sup>C. K. N. Patel and R. E. Slusher, Phys. Rev. Lett. **20**, 1087 (1968).
- <sup>7</sup>S. S. Alimpiev and N. V. Karlov, Zh. Eksp. Teor. Fiz. **63**, 482 (1972) [Sov. Phys. JETP **36**, (1973)].
- <sup>8</sup>S. S. Alimpiev, Dissertation, Phys. Inst. Acad. Sci. SSSR, 1973; Tr. Fiz. Inst. Akad. Nauk SSSR **87**, 92 (1976).
- <sup>9</sup>J. R. Meckley and C. V. Heer, Phys. Lett. **46A**, 41 (1973).
- <sup>10</sup>R. J. Nordstrom, W. M. Gutman, and C. V. Heer, Phys. Lett. **50A**, 25 (1974).
- <sup>11</sup>W. M. Gutman and C. V. Heer, Phys. Lett. **51A**, 437 (1975).
- <sup>12</sup>V. V. Samartsev and V. R. Nagibarov, Fiz. Tverd. Tela (Leningrad) **11**, 3669 (1969) [Sov. Phys. Solid State **11**, 3085 (1970)].
- <sup>13</sup>A. I. Alekseyev, Phys. Lett. **31A**, 495 (1970).
- <sup>14</sup>G. Oliver and R. Lefebvre, J. Phys. (Paris) **31**, 761 (1970).
- <sup>15</sup>S. M. Zakharov and E. A. Manykin, Zh. Eksp. Teor. Fiz. **60**, 1867 (1971) [Sov. Phys. JETP **33**, 1009 (1971)].
- <sup>16</sup>A. I. Alekseev and I. V. Evseev, Abstracts, 2nd All-Union Symp. on Gas-Laser Physics, Novosibirsk, 1975, p. 71.
- <sup>17</sup>A. I. Alekseev and A. M. Basharov, Zh. Eksp. Teor. Fiz. **74**, 1988 (1978) [Sov. Phys. JETP **47**, 1035 (1978)].
- <sup>18</sup>I. I. Sobel'man, Vvedenie v teoriyu atomnykh spektrov (Introduction To the Theory of Atomic Spectra), Nauka, 1977.

Translated by J. G. Adashko

## Laser fluorescence detection of single atoms

V. I. Balykin, V. S. Letokhov, and V. I. Mishin

*Spectroscopy Institute, USSR Academy of Sciences*

(Submitted 30 May 1979)

Zh. Eksp. Teor. Fiz. **77**, 2221-2237 (December 1979)

Results are presented of an investigation of the detection of single sodium atoms by means of a fluorescence method under conditions of cyclic interaction between the sodium atoms and a circularly polarized light wave of resonant frequency. To ensure multiple interaction between the atoms and laser radiation, the atoms are preliminarily oriented optically, as a result of which they occupy the  $F = 2$ ,  $m_F = 2$  sublevel from which only a transition to the  $F' = 3$ ,  $m'_F = 3$  sublevel is possible. The maximum mean signal from each sodium atom interacting with the radiation is  $\bar{n}_{\max} = 2$  photoelectrons. The minimum recorded sodium atom flux in the experiment is  $\approx 1$  atom/sec for an atomic registration probability of 0.4. Strong suppression of the atomic absorption spectral line wings occurs on registration of single atoms when the fluorescence signal in the center of the absorption line is  $\bar{n}_{ph} > 1$  photoelectron. It is shown that this method of suppression of spectral line wings can be used to detect low concentrations of the atoms of a certain element in the presence of a high concentration of another element when the distance between the spectral absorption lines of the elements is  $\approx 0.1-100 \text{ cm}^{-1}$ .

PACS numbers: 32.50. + d, 35.80. + s

### INTRODUCTION

One of the pressing problems in the development of laser spectroscopy methods is the attainment of maximum sensitivity, up to a limit of spectroscopy of quan-

tum states using single atoms and molecules.<sup>1,2</sup> In investigations of ultrasmall concentrations of atoms, the most effective are the fluorescence and photoionization methods, which have yielded the best results. Using cw dye lasers and a standard fluorescence pro-

cedure, it was possible in Refs. 3 and 4 to detect sodium atoms with a minimum concentration down to  $10^2$  atoms/cm<sup>2</sup> and uranium atoms with a minimum concentration  $3 \times 10^3$  atoms/cm<sup>3</sup> ( $\sim 10$  atoms in the registration zone). An improvement of this method has made it possible to advance to a registration of individual atoms, as was done for sodium atoms<sup>5,6</sup> and barium atoms.<sup>7</sup> The stepwise photoionization method proposed<sup>1,2,8,9</sup> for the detection of atoms made possible the detection of single atoms of Cs,<sup>10</sup> Na,<sup>11</sup> and Yb.<sup>12</sup>

In the present paper we present the results of an investigation of the detection of single Na atoms by a fluorescent method under conditions of controlled cyclic interaction of Na atoms with a circularly polarized laser light wave at the resonant frequency.

## 2. FORMULATION OF PROBLEM

A feature of the method of resonant fluorescence is that the same atom can interact, under certain conditions, many times with the laser radiation and scatter resonantly the spontaneous-emission of photons. Repeated interaction of an atom with laser radiation is realized under the following conditions:

- 1) cyclic character of the interaction of the same atom with the laser radiation at resonance;
- 2) saturation of the cyclic quantum transition by sufficiently intense laser radiation.

The first condition ensures multiple resonance between the frequency of the laser radiation and a definite pair of levels of the atom during the time of interaction when the photons are reradiated. The second condition ensures a sufficient number of reradiated photons for reliable registration.

Several methods of realizing a cyclic interaction of the atom with the radiation can be indicated. The simplest case is when the atom levels interacting with the laser radiation can be represented by a two-level scheme. Examples are atoms in which the resonant transition is not split by hyperfine interaction (Na<sup>20</sup>, Ba). This case, however, is rare. An atom having a hyperfine structure can be brought into one of the hyperfine-structure states from which it interacts with the radiation like a two-level system.<sup>13,14</sup> The most general case of realization of a cyclic interaction is through the use of several transitions excited by a multifrequency laser.

In the present study, using sodium, which has a hyperfine structure, the cyclic interaction was effected by the second method between the atom and circularly polarized laser radiation.

Figure 1a shows the energy scheme of the hyperfine structure of the  $D_2$  line of the sodium atom. The only transition that satisfies the multiple excitation condition is  $3^2S_{1/2}(F=2) \rightarrow 3^2P_{3/2}(F'=3)$ , so that in accordance with the selection rules the atom can go from the  $F'=3$  state only to a lower state with  $F=2$ . Thus cyclic excitation of the atom can be produced by a

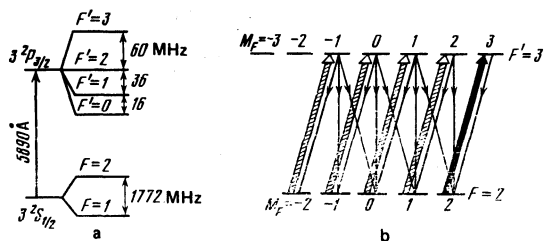


FIG. 1. a) Energy diagram of hyperfine structure of the  $D_2$  line of the Na atom; b) optical orientation of the Na atom by circularly polarized laser radiation.

single-mode cw dye laser whose frequency stability in time does not exceed the homogeneous absorption line width. As noted above, to obtain the maximum number of scattered photons from a single atom it is necessary that the power of the exciting radiation exceed the saturation power. In this case, however, a noticeable broadening of the levels takes place<sup>13</sup> and leads to transitions of the atoms from the lower state  $3^2S_{1/2}(F=2)$  to an upper state  $3^2P_{3/2}(F'=2)$ , from which it can go over to the ground state with  $F=1$ . In this state the atom can no longer interact with the laser radiation because of the large frequency difference between the components  $F=1$  and  $F=2$ . The excitation ceases to be cyclic as a result.

In Refs. 5 and 6, cyclic excitation of the atom was produced by using a multimode dye laser at high power ( $\approx 150$  mW) a resulting in a noticeable broadening and overlap of the hyperfine splitting levels of the upper state  $F'=3$ . The atoms were excited both from the sublevel  $F=2$  and from the sublevel  $F=1$  of the ground state.

In the present study, to obtain a cyclic interaction between the radiation and the atom, the sodium atom was first optically oriented (Fig. 1b). Intense  $\sigma^+$ -polarized light excites transitions with change of the magnetic quantum number  $\Delta m = +1$ . As a result of this process, the atoms are optically pumped into the state  $F=2, m_F=2$ . The only transition possible from this state is to an upper state with  $F'=3, m'_F=2$ . Transitions from the state with  $F'=2, m'_F=-2, -1, 0, +1, +2$  are also forbidden in the dipole approximation. Thus, the atoms in the state  $F=2, m_F=2$  can be regarded as two-level systems in which multiple cyclic excitation is possible.

It should be noted that even in this case there are channels through which the atom excitation can lose its simplicity. First, in optical pumping, when not all the atoms are gathered on the sublevel  $F=2, m_F=2$ , transitions to upper states with  $F'=2$  are possible, followed by a transition to the ground state with  $F=1$ . Second, regardless of the method used to obtain  $\sigma^+$ -polarized laser radiation, a fraction of the radiation is always linearly polarized. As will be shown below, neither of these channels is significant in our case.

Let the atom cross a laser beam tuned to a resonant absorption line. Then, in the regime of cyclic interaction of the atom with the laser radiation, during the time that the atom crosses the beam it absorbs and emits a number of photons, equal to

$$N = \frac{t_c A_{21}}{1 + 1/\eta} = \frac{t_c}{\tau_{21}(1 + 1/\eta)}, \quad (1)$$

where  $A_{21}$  and  $\tau_{21}$  are respectively the Einstein coefficient of the considered transition and the lifetime of the upper level,  $\eta$  is the ratio of the average populations of the upper and lower levels, and  $t_c$  is the time of cross of the beam by the atom. If the intensity of the laser radiation exceeds the intensity of the saturation of this transition, then the number of emitted photons is

$$N_{\max} = t_c / 2\tau_{21}. \quad (2)$$

We now estimate this time for the sodium atom. The most probable velocity of the sodium atom at a temperature 50°C in an atomic beam is  $5.8 \times 10^4$  cm/sec. The lifetime of the excited state is  $\tau = 1.6 \cdot 10^{-8}$  sec. Then the number of photons emitted by the atom over a path of 4 mm in the laser beam is 220. The use of an ellipsoidal reflector makes it actually possible to gather on the photomultiplier cathode photons from a solid angle of approximately 5 sr. The number of photons incident on the photo-cathode is then  $N_{\text{det}} \approx 90$ . The better photomultipliers have a quantum efficiency 10–20% at a wavelength  $\lambda = 589.0$  nm.

Thus, from each passing atom whose excited transition is in the deep-saturation regime one can expect from the photomultiplier cathode a maximum signal  $N_{\text{at}} \approx 9$  photoelectrons.

In the resonance-fluorescence method, the sensitivity is limited by the background signal due to the scattering of the laser radiation by the parts of the cell in which the atoms are detected. The background radiation incident on the photocathode during the time that the atom crosses the laser beam is

$$N_b = \xi W_L t_c / h\nu, \quad (3)$$

where  $W_L$  is the laser-emission power at the entry to the cell, and  $\xi$  is a parameter that characterizes the quality of the cell and is equal to the ratio of the stray laser radiation incident on the photocathode to the laser power at the entry to the cell.

The necessary condition for observing an atom is the requirement

$$N_b \ll N_{\text{det}}. \quad (4)$$

From this requirement we can estimate the value of:

$$\xi \ll N_{\text{det}} h\nu / W_L t_c. \quad (5)$$

For the experiment described above  $W_L = 10^{-3}$  W,  $T = 12$   $\mu$ sec, and condition (5) yields  $\xi \ll 2 \times 10^{-9}$ .

### 3. EXPERIMENTAL SETUP AND RECORDING PRINCIPLE

The experimental setup is illustrated in Fig. 2. It consists of the following principal elements: a laser atom-excitation source, a cell in which the radiation interacts with the atom, an atom source, recording and analyzing electronic circuitry, and a system for monitoring the frequency and power of the excited radiation.

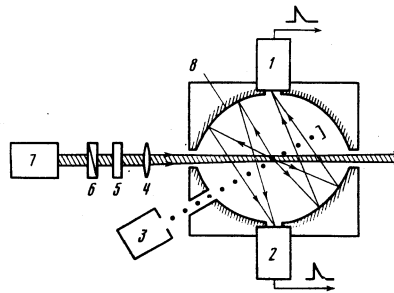


FIG. 2. Diagram of experimental setup: 1, 2—photomultipliers, 3—atomic-beam source, 4—lens, 5— $\lambda/4$  plate, 6—Glan prism, 7—laser, 8—ellipsoid.

The source of excitation of the sodium atoms was a single-mode cw dye laser. The radiation power reached 10 mW. The lasing frequency could be tuned to the axial modes of the resonator ( $\Delta\nu_M = 400$  MHz). To obtain circularly polarized ( $\sigma^+$ ) radiation, the laser beam was passed in succession through a polarizer (Glan prism) and a quartz quarter-wave plate. The degree of polarization was not worse than 99%. The radiation was applied to a cell with a sodium-atom beam. The cell was designed to minimize the stray light. For this purpose it was blackened, diaphragms of variable diameter were placed outside and inside, and the entrance windows had surfaces with small light scattering coefficients. The cell was evacuated to  $10^{-4}$  Torr. To saturate the excited transition at a small laser input power and to decrease the background signal due to the laser beam as it passed through the internal diaphragms of the cell, the laser radiation was focused with a long-focused lens ( $F = 50$  cm). The beam diameter in the interaction region was  $d = 0.57$  mm. Since the laser radiation was single-mode and could be tuned only in discrete steps equal to the distance between the longitudinal resonator mode ( $\Delta\nu_M = 400$  MHz), the tuning to the transition  $3^2S_{1/2}(F=2) \rightarrow 3^2P_{3/2}(F'=3)$  was effected by directing the atom beam at an angle to the laser beam. The source of the sodium vapor was an oven in which metallic sodium was placed. The oven temperature could range from room temperature to 100°C. The atom beam was collimated by a cylindrical channel 4 mm long and 0.5 mm in diameter and by additional diaphragms. The distance from the split of the oven to the interaction region was 150 mm. The atom beam crossed the laser beam at an angle 7°. The average path of the atom in the beam was 4 mm.

The resonant fluorescence was gathered by two ellipsoids so arranged that the atoms interacting with the laser beam were located in one of the foci of the ellipsoids and the cathodes of the photomultipliers (FÉU-79) were located in the other focus. The gathering angle of one ellipsoid was  $\Omega = 4.6$  sr. The selected photomultipliers were those having the maximum quantum yield out of a large batch.

The use of elliptic reflectors to increase the number of photons coming from the atom resulted in the present study to an increase of the laser stray light incident on the photocathode, compared with the case

when a cell with lens condensers is used.<sup>5,6</sup> The parameter  $\xi$  characterizing the quality of the cell increased from  $10^{-14}$  to  $6 \times 10^{-12}$ . For the described experiment, the input power was  $I \leq 10^{-3}$  W,  $T = 12$   $\mu$ sec, and condition (5) was certainly satisfied:  $\xi_{\text{exp}} \ll 2 \times 10^{-9}$ .

At the indicated laser-radiation input power and the parameter  $\xi$ , the background radiation incident on the photomultiplier cathode during the time of flight of the atom through the beam amounts to 0.3 photon, which is negligibly small compared with the signal from the atom.

To register the atoms we chose a system with double coding, in which a signal was registered when the number of electrons from the photomultiplier cathode, during the measurement time, was equal to or larger than the discrimination threshold, and no signal was registered at a lower number. In such a system, in the absence of a background signal, passage of an atom is registered if at least one photoelectron is received during the measurement time (in our case, during the time of flight of the atom through the laser beam). On the other hand if not a single photoelectron is received, absence of an atom is registered.

In the real situation, photoelectrons produced by the background due to the stray laser radiation and to the dark current of the photomultiplier are present. This makes it necessary to increase the registration threshold compared with a value equal to one photoelectron during the measurement time. Because of the statistical character of the photon emission by the atom, the increase of the registration threshold makes it possible that a signal (atom) can remain unobserved. The background results not only in the need for increasing the threshold, but also in the appearance of a false signal.

Assuming that the photoelectrons have a Poisson distribution the expression for the probability of receiving a signal is<sup>15</sup>

$$P_s = \sum_{m=n_t}^{\infty} \frac{\bar{n}_s^m}{m!} \exp(-\bar{n}_s), \quad (6)$$

where  $n_s$  is the average number of photoelectrons during the time of registration in the presence of a signal, and  $n_t$  is the threshold level above which the received signal is registered. The probability of receiving a false signal is given by

$$P_{\text{false}} = \sum_{m=n_t}^{\infty} \frac{\bar{n}_b^m}{m!} \exp(-\bar{n}_b), \quad (7)$$

where  $n_b$  is the average number of the background photoelectrons.

Figure 3 shows the electric block diagram of the setup that made it possible, during the time of the experiment, first, to analyze the number of pulses arriving during the strobing time, i.e., the number of photoelectrons arriving during the time of flight of the atom through the laser beam; second, to provide discrimination with respect to the number of received photoelectrons during the strobing time, so as to eliminate the background parasitic signal; and third,

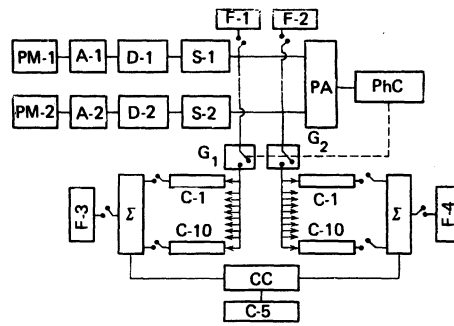


FIG. 3. Electric block diagram (the symbols are explained in the text).

to provide time discrimination with the aid of a coincidence circuit for additional elimination of the background signal and to determine the atom registration probability.

The pulses from the photomultiplier were fed respectively to amplifiers (U-1,2), discriminators (D-1,2) and pulse shapers (S-1,2). After shaping, the pulses were fed to an adder (PA) and gates G-1, G-2, which were closed in the normal state. The first pulse received by the adder triggers the shaper of the strobing signal, whose duration could be varied in the range from 3 to 60  $\mu$ sec. The strobing duration in the experiment was chosen to be equal to the average time of flight of the atom through the laser beam. The strobing signal opened the gates G-1 and G-2 and the pulses from each channel were fed, during a time equal to the strobing duration, to counters C-1, ... C-10. Each of the ten counters operated after receiving a number of pulses equal to the number of the counter. The signals from the counter were fed to the adder  $\Sigma$ , whose function was to generate a signal if it received at least one pulse from the counters C-1, ... C-10. The pulses proceeded from the adder either to frequency meters F-3, F-4, or to a coincidence circuit CC, from which they were fed in turn to the frequency meter F-5. Frequency meters F-1, and F-2 were intended to count the pulses in each of the channels.

#### 4. OPTICAL ORIENTATION AND CYCLICITY OF EXCITATION OF THE ATOM

The crucial instant in fluorescent detection of atoms is the realization of cyclic excitation of the atom, so as to obtain the maximum number of photons during the time of flight of the atom through the laser beam. In the present study this was accomplished by optically orienting the sodium atom, so that the atom landed in the state  $3^2S_{1/2}(F=2, m_F=2)$ , became a two-level system, and could absorb and emit repeatedly photons via the transition  $F=2, m_F=2 \rightarrow F'=3, m_{F'}=3$ .

In the experiment, the atom beam was directed at a small angle to the laser beam, so that the first to interact with the laser beam, inasmuch as the sodium atom has a hyperfine structure, are three groups of atoms from the Doppler contour in a small range of velocities, for which the condition of resonance with

the radiation is satisfied. These three groups of atoms are excited from the ground state with  $F=2$  into excited states with  $F'=3, 2, 1$ . All the atoms excited into states with  $F'=2$  and 1 go over very rapidly, compared with the time of stay of the atom in the laser beam, into the state with  $F=1$  and no longer interact with the laser radiation. This group of atoms will not be considered hereafter.

The atoms whose transition  $F=2 \rightarrow F'=3$  has a frequency resonant with the laser radiation, can interact repeatedly with the radiation. The intense circularly-polarized laser radiation excites transitions with  $\Delta m = +1$ ; as a result of these transitions, the atoms reach very rapidly the sublevel  $F=2, m_F=2$ .<sup>13</sup> The only possible transition from the sublevel  $F=2, m_F=2$  is to the sublevel  $F'=3, m_{F'}=3$ . The nonresonant transitions  $F=2, m_F=2 \rightarrow F'=2, m_{F'}=-2, -1, 0, +1, +2$ , are also forbidden by the selection rules. Thus, when the atom is on the sublevel  $F=2, m_F=2$ , it can repeatedly and cyclically interact with the circularly polarized ( $\sigma^+$ ) laser radiation.

In the course of the optical pumping, however, the interaction of the atom with the laser radiation can be interrupted by nonresonant transitions from the sublevel  $F=2, m_F=-2, -1, 0, +1$  to the sublevels  $F'=2, m_{F'}=-2, -1, 0, +1, +2$ , from which the atom can go over to a lower sublevel with  $F=1$  and cease to interact with the laser radiation.

Calculations of the distribution of the calculations of the sublevels of the  $3^2S_{1/2}$  state of the sodium atoms in the atom beam optically pumped by laser radiation with  $\sigma^+$  polarization and linear polarization ( $\pi$ ) were calculated under the following assumptions: 1) the laser radiation is at resonance with the transition  $F=2 \rightarrow F'=3$ ; 2) the transitions to the nearest sublevel of the upper state  $F'=2$  is due to the wing of the absorption line; 3) the transitions from the level  $F=1$  to the level  $F'=2$  are inessential and therefore disregarded; 4) the magnetic substructure of the levels  $F=1$  is disregarded. Thus, we consider the following lower-state levels:

$$F=1, (F, m_F) = (2, -2), (2, -1), (2, 0), (2, +1), (2, +2)$$

and the following upper-state levels: a) for  $\sigma^+$  polarization:

$$(F', m_{F'}) = (3, -1), (3, 0), (3, +1), (3, +2), (3, +3), (2, -1), (2, 0), (2, 1), (2, 2)$$

and b) for  $\pi$  polarization:

$$(F', m_{F'}) = (3, -2), (3, -1), (3, 0), (3, +1), (3, +2), (2, -2), (2, -1), (2, 0), (2, 1), (2, 2).$$

The kinetic equations for the populations of the considered sublevels are of the form

$$\frac{dn_k}{dt} = -n_k \sum_j w_{kj}^\beta + \sum_i n_i' (w_{ik}^{\beta'} + A_{ik}^{\beta'}) \quad (8')$$

for the lower levels and

$$\frac{dn_k'}{dt} = -n_k' \sum_j (w_{kj}^{\beta'} + A_{kj}^{\beta'}) + \sum_i n_i w_{ik}^\beta \quad (8'')$$

for the upper levels, where we have put  $\beta \equiv F, m_F$ ;  $\beta' \equiv F', m_{F'}$ . Here  $n_k$  and  $n$  are the populations of the

lower and upper levels;  $A_{kj}^{\beta'}$  are the probabilities of the spontaneous transition between levels;  $w_{ik}^\beta$  and  $w_{kj}^{\beta'}$  are the probabilities of stimulated transitions:

$$w_{ik}^\beta = I_0 B_{ik}^\beta \int_{-\infty}^{\infty} \alpha(v-\delta-v_0) g(v-v_0) dv, \quad (9)$$

where  $I_0$  is the integrated intensity of the laser radiation and  $B_{ik}^\beta$  is the Einstein coefficient of the stimulated transition. It is assumed that the spectral profile of the laser radiation is

$$g(v-v_0) = \left(\frac{4}{\pi} \ln 2\right)^{1/2} \frac{1}{\Delta\nu_L} \exp\left[-4 \ln 2 \left(\frac{v-v_0}{\Delta\nu_L}\right)^2\right], \quad (10)$$

$$\int_{-\infty}^{\infty} g(v-v_0) dv = 1, \quad (11)$$

where  $\Delta\nu_L$  is the width of the laser-emission line. The absorption-line contour is

$$\alpha(v-\delta-v_0) = \frac{1}{\pi} \frac{\Delta\nu_{\text{hom}}/2}{(v+\delta-v_0)^2 + (\Delta\nu_{\text{hom}}/2)^2}, \quad (12)$$

$$\int_{-\infty}^{\infty} \alpha(v-\delta-v_0) dv = 1,$$

where  $\Delta\nu_{\text{hom}}$  is the homogeneous width of the sodium-atom absorption line and  $\delta$  is the frequency difference between the center of the absorption line and the central frequency of the laser emission.

Figure 4a shows the calculated plots of the populations of the  $F'=3$  levels in the interaction with radiation of power  $I_0 = 100 \text{ mW/cm}^2$  and  $\Delta\nu_L = 10 \text{ MHz}$  with circular  $\sigma^+$  polarization and linear  $\pi$  polarization as functions of the time of interaction with the radiation. The population of the level  $F'=3$  in interaction with  $\sigma^+$  polarized radiation is increased by optical pumping; when the optical pumping ends, the population of the level remains practically constant in time. When the atom interacts with  $\pi$  polarized radiation there is no optical pumping to the sublevel  $F=2, m_F=2$ , and the atom goes over via non-resonant interaction with the upper level  $F'=2$  to the lower level  $F=1$ . The population of the level  $F'=3$  decreases continuously during the time of flight of the atom through the laser beam.

A similar difference in the behavior of the populations of the level with  $F'=3$  should lead to a change in the fluorescence signal from the atoms interacting with

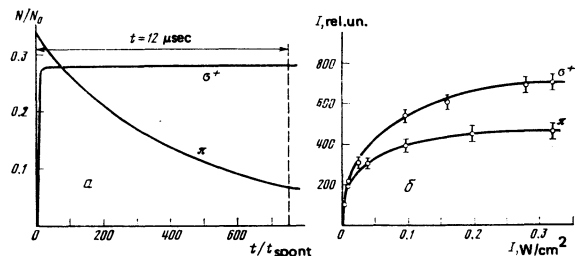


FIG. 4. Optical orientation of sodium atom. a) time variation of population of the sublevel  $3^2P_{3/2}$  ( $F'=3$ ) when atoms interact with  $\sigma^+$  and  $\pi$  polarized radiation whose frequency is tuned to resonance with the transition  $3^2S_{1/2}$  ( $F=2$ )  $\rightarrow$   $3^2P_{3/2}$  ( $F'=3$ ) ( $I_0 = 100 \text{ mW/cm}^2$ ,  $\Delta\nu = 10 \text{ MHz}$ ), b) dependence of the fluorescence signal of Na atoms on the laser-radiation power for the two polarizations  $\sigma^+$  and  $\pi$ .

$\sigma^*$  and  $\pi$  polarized radiation, since the integral of the dependence of the atom population on the  $F'=3$  level is proportional to the fluorescence signal from the atom. From the difference between the values of the fluorescence signal one can assess the degree of polarization of the atom.

Figure 4b shows plots of the fluorescence from the sodium atom in the beam when  $\sigma^*$  and  $\pi$  polarized radiation excited the transition  $3^2S_{1/2}(F=2) - 3^2P_{3/2}(F'=3)$ . It is seen from the figure that with increasing laser power the absorption of the transition saturates in both polarizations. The fluorescence signal following excitation with  $\sigma^*$  polarized radiation exceeds the fluorescence signal due to  $\pi$  polarization excitation by a factor 1.52 and a power  $300 \text{ mW/cm}^2$ . Comparing this value with the ratio 1.68 of the integrals of the curves that describe the population on the level  $F'=3$  in Fig. 4a, we can conclude that the sodium atoms are effectively oriented.

Optical pumping should lead to a change in the ratio of the fluorescence signals when the laser is tuned to the transitions  $3^2S_{1/2}(F=2) - 3^2P_{3/2}(F'=3)$  and  $3^2S_{1/2}(F=1) - 3^2P_{3/2}(F'=1,2)$ , as a function of the laser radiation power. Tuning to the first transition should cause optical orientation of the atom, and tuning of the laser radiation to the second transition cannot orient the atom in our case.

Figure 5 shows the absorption-line contours of the atoms in the beam when the laser radiation is scanned, for three different values of the laser power. It is seen that at low radiation power ( $I_L = 0.2 \text{ mW/cm}^2$ , Fig. 5a) the ratio of the intensities of the hyperfine structure components corresponds to the statistical weights of the levels and is equal to 1.68. When the pump power is increased ( $I_L = 7.8$  and  $660 \text{ mW/cm}^2$ , Figs. 5b and 5c) the fluorescence signal corresponding to the transition from  $F=2$  of the ground state increases strongly, thus indicating that atoms are

accumulated on the sublevel  $F=2, m_F=2$ , i.e., the atoms become optically oriented.

## 5. REGISTRATION OF MULTIPHOTOELECTRON PULSES

The number of photons emitted by each atom as it passes through the laser beam is a random quantity and is described by a Poisson distribution. The statistics of the photoelectron emission is also described by a Poisson distribution. By repeating many times the experiment on the reception of the signal from the sodium atoms passing through the laser beam and interacting with the radiation (as was in fact done in the experiment) it is possible to find this distribution. Not only the distribution of the number of photoelectrons it is possible to turn to determine the average number of photoelectrons from the atom. Knowledge of the average value of the received photoelectrons from the atom is essential when it comes to discriminating the parasitic background, and also for many other applications which will be discussed later on.

It should be noted that an important role in the determination of the average value of the photoelectrons from an atom is played by the estimate of the fluctuations of the atom flux itself, neglect of which can distort the determined quantity. At the atomic-beam geometry used in the experiment, and at an oven temperature,  $T = 90^\circ \text{C}$  (the maximum oven temperature used in the measurements) it is easy to estimate that the flux through the interaction zone is  $N = 2 \times 10^5$  atoms/sec. The actual number in the experiment was smaller because of scattering of the atomic beam in the residual gas of the cell ( $p = 10^{-4}$  Torr). Since the laser beam interacts only with the group of atoms from the Doppler contour in a small range of velocities corresponding to the homogeneous absorption-line width, the flux of the interacting atoms amounts to  $N_{\text{at}} = N \Delta v_{\text{hom}} / \Delta v_{\text{Dop}} = 2.5$  atoms/sec. At a strobing duration  $\tau = 12 \mu\text{sec}$ , the average number of atoms in the interaction volume is  $\bar{N}_{\text{max}} = 0.03$ . The probability of two atoms landing in this volume during the time of interaction can be easily estimated from the Poisson formula and amounts to  $P(2) = 4.5 \cdot 10^{-4}$ . The probability of 3, 4 and more atoms landing there is even smaller, i.e., such event can be neglected both when considering the fluctuations of the photoelectrons and when measuring the velocity of the flux of atoms.

Figure 6 shows the dependence of the number of registered pulses from the flux of the sodium atoms interacting with the radiation on the discrimination threshold during a measurement time  $t = 1$  at a strobe duration  $t = 12 \mu\text{sec}$  and at a laser radiation intensity  $I_L = 120 \text{ mW/cm}^2$ . The discrimination threshold  $n_t = 1$  corresponds to registration of atoms producing a signal equal to one and more photoelectrons, the threshold  $n_t = 2$  is the same for two or more photoelectrons, etc. The maximum discrimination threshold at which atoms could still be detected as  $n_t = 8$ . The experimental points are best approximated by a Poisson distribution with  $\bar{n} = 1.3$ , i.e., the average number of photoelectrons received from the atom is 1.3.

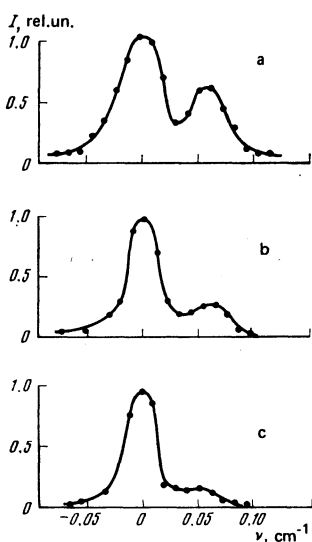


FIG. 5. Change of the contour of the  $D_2$  line of sodium atoms interacting with  $\sigma^*$  polarized laser radiation: a)  $I_L = 0.2 \text{ mW/cm}^2$ , b)  $I_L = 7.8 \text{ mW/cm}^2$ , c)  $I_L = 660 \text{ mW/cm}^2$ .

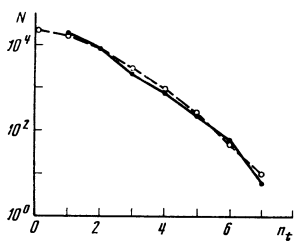


FIG. 6. Number of registered pulses from a beam of sodium atoms interacting with radiation as a function of the discrimination threshold (●). Dashed curve—Poisson distribution function with  $\bar{n}_0 = 1.3$  (○).

Figure 7 shows the ratio of the number  $N_{\text{coin}}$  of the pulses received from the sodium atoms and registered by the coincidence circuit to the number  $N_1$  of the pulses registered in one channel, as a function of the laser-radiation power. At a low laser power,  $I_L < I_{\text{sat}}$ , the ratio  $N_{\text{coin}}/N_1$  is much less than unity, i.e., the signal in one channel is larger than in the coincidence circuit. The reason is that at low radiation power the sodium atom passing through the laser beam does not emit enough photons to record it simultaneously in both channels. If the probability of the registration of the atom in one channel is  $P_1$ , then the probability of its registration in the coincidence circuit is  $P_{\text{coin}} = P_1^2$ . When the laser power is increased, the probability of registration of the atom increases. The number of registered atoms in one channel is  $N_1 = N_{\text{at}} P_1$ , where  $N_{\text{at}}$  is the number of atoms interacting with the radiation. The number of registered atoms in the coincidence circuit is  $N_{\text{coin}} = N_{\text{at}} P_{\text{coin}} = N_{\text{at}} P_1^2$ . From these two expressions we get for the probability of registering an atom  $P_1 = N_{\text{coin}}/N_1$ . From the plot in Fig. 7 we can determine the probability of registering an atom:  $P_1 = 0.87$ , i.e., at a power  $I_L \gg I_{\text{sat}} = 10$  mW/cm<sup>2</sup> the probability of registering an atom in our case is 87%. Knowing the probability of registration of an individual atom at a discrimination threshold  $n_t = 1$ , we can determine from (6) the maximum average number of photoelectrons received from the atom. The sum in the right-hand part of expression (6) was tabulated for different values in Ref. 16. Using the data of that reference and the atom-registration probability  $P_1 = 0.87$ , we get for the average number of photoelectrons  $n = 2$ . This is smaller by a factor 4.5 than the value estimated in the introduction. The principal causes of the loss of photons emitted by the atom are the following: the decrease of the reflection

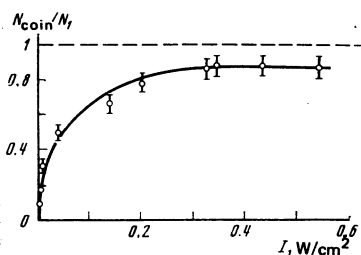


FIG. 7. Ratio of the number of registered pulses from a beam of sodium atoms in one channel ( $N_1$ ) to the number of registered pulses in the coincidence circuit ( $N_{\text{coin}}$ ) as a function of the laser-radiation.

coefficient of the peripheral regions of the ellipsoids, the losses in the focusing on the photomultiplier cathodes, and the insufficient quantum efficiency of the photomultipliers.

## 6. REGISTRATION OF SINGLE ATOMS

After selecting the atom-registration regime (power, spectrum, radiation polarization) that yields a maximum registration probability we registered the atom flux while varying the oven temperature. Figure 8 shows the dependence of the atom flux registered in the coincidence circuit on the oven temperature at the various discrimination thresholds. The upper plot was obtained at  $n_t = 1$  (all the atoms that produce a signal of one photoelectron and more are registered), and the lower plot at  $n_t = 2$  (all the atoms that produce a signal of 2 photoelectrons and more). It is seen that at  $n_t = 1$  the minimum registered atom flux is determined by the background stray illumination and amounts to approximately 200 atoms/sec. The probability of registration of each atom is in this case  $P = 0.8$ .

At a discrimination threshold  $n_t = 2$ , the background signals is decreased and the sensitivity of the system correspondingly increased. In this case the minimum registered atom flux amounts to several atoms per second. However, at the same time the probability of registration of the atoms decreases to  $P = 0.4$ .

Figure 9 shows plots of the atom registration probability against the discrimination threshold for different values of the average number of registered photoelectrons, calculated from formula (6). It is seen from the figure that the discrimination level that can be used for the registration of the atoms depends substantially on the average number of photoelectrons. The larger this number, the higher the discrimination threshold that can be effected for the registration of

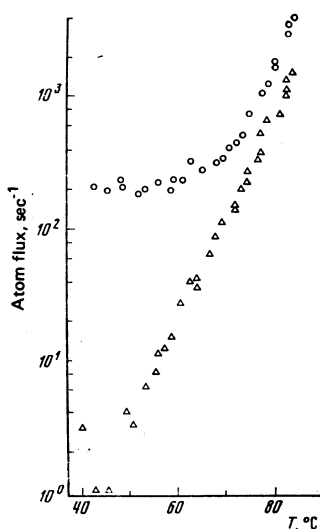


FIG. 8. Atom flux as a function of the oven temperature for different discrimination thresholds: ○— $n_t = 1$  ( $P = 0.8$ ), △— $n_t = 2$  ( $P = 0.4$ ).

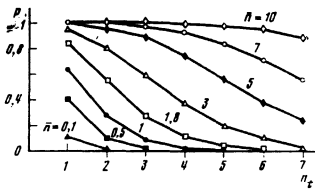


FIG. 9. Atom—registration probabilities as functions of the discrimination threshold at different values of the average number of the registered photoelectrons from the atom.

an atom without substantially decreasing the registration probability.

## 7. MULTIPHOTOELECTRON SPECTROSCOPY

It is seen from Fig. 9 that the probability of registration of the atom at a definite discrimination threshold is larger the larger the mean value of the photoelectrons received from the atom. When the laser frequency is tuned away from the center of the absorption line of the atom, the average number of photoelectrons that can be registered from the atom decreases with the decrease of the absorption cross section. This leads to a decrease of the probability of registration of an atom when the frequency of the laser is tuned to the absorption-line wing. When the atom flux is registered, the signal at the center of the absorption line ( $\nu_L = \nu_0$ ) is equal to  $N_0 = N_{at}P(0)$ , where  $N_{at}$  is at the flux of the atoms interacting with the radiation and  $P(0)$  is the probability of registration of the atom at  $\nu_L = \nu_0$ . At a laser frequency  $\nu_L = \nu_0 + \Delta\nu$ , on the absorption-line wing, the corresponding signal is  $N = N_{at}P(\Delta\nu)$ , where  $P(\Delta\nu)$  is the probability of registration of an atom when the frequency of the laser is detuned from the center of the absorption line by  $\Delta\nu$ .

Assume that the number of received photoelectrons is discriminated in the course of the detection of the atom. If the number of photoelectrons at the center of the absorption line (i.e., at  $\nu_L = \nu_0$ ) is  $\bar{n} \geq 1$ , then this discrimination does not lead to a noticeable decrease of the probability of registration of the atom, meaning also the signal  $N_0$ . At a noticeable deviation of the laser frequency from the absorption-line center, the number of photoelectrons received from the atom decreases substantially and the atom registration probability is correspondingly decreased. Discrimination in this case lowers noticeably the atom registration probability  $P(\Delta\nu)$ , meaning also the magnitude of the signal  $N$ . Thus, in this atom-registration regime one should observe a strong suppression of the spectral-line wings.

Figure 10 shows the beam-atom absorption-line contours measured in the indicated regime. The average number of photoelectrons in this case is  $n_0 = 1.8$ . The discrimination threshold changed from 1 to 4. The figure shows the suppression of the absorption-line wings when the discrimination threshold is increased. The magnitude of the wing suppression can be characterized by the detection selectivity defined as

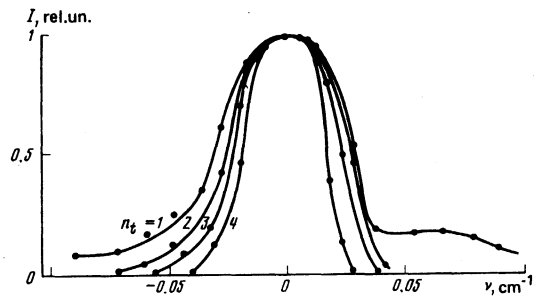


FIG. 10. Dependence of the absorption-line contour of Na atoms in a beam, corresponding to the transition  $3^2S_{1/2}(F=2) \rightarrow 3^2P_{3/2}(F'=3)$ , in cyclic interaction of the atoms with the laser radiation.

$$S_{n_x}(\nu) = \frac{P(0)}{P(\Delta\nu)} = \frac{\sum_{m=n_x}^{\infty} \frac{\bar{n}_0^m}{m!} \exp(-\bar{n}_0)}{\sum_{m=n_x}^{\infty} \frac{\bar{n}^m}{m!} \exp(-\bar{n})}. \quad (13)$$

It is equal to the ratio of the probability of registering the atom at  $\nu_L = \nu_0$  at the center of the absorption line to the registration probability on the absorption-line wing at the frequency  $\nu_L = \nu_0 + \Delta\nu$ . It is easily seen that the detection selectivity defined in this manner is equal to

$$S_{n_x} = \frac{P(0)N_{at}}{P(\nu)N_{at}} = \frac{N_0}{N} \Big|_{n_x}, \quad (14)$$

which is the ratio of the signal at the center of the absorption line to the signal at the frequency  $\nu_0 + \Delta\nu$  for the chosen discrimination threshold.

Figure 11 shows the selectivity of detection of the sodium atom as a function of the discrimination threshold, obtained from the plot of Fig. 10 for a frequency deviation  $\Delta\nu = 0.036 \text{ cm}^{-1}$  from the center of the absorption line. The selectivity was determined from (14). The dashed curve in the same figure shows a calculated detection selectivity obtained from formula (13) at  $\bar{n}_0 = 1.8$ , taken from an experiment in which the absorption line contour was measured in the multiphoto electron registration regime. The two plots agree within the limits of errors.

The excitation selectivity  $S_{n_x}(\nu)$  describes not only the degree of suppression of the spectral-line wings, but also the detecting ability when the concentration of one element is determined against the background of the concentration of another element. For example, if the number of excitation cycles of two different atoms (elements, isotopes, excited isomers) with

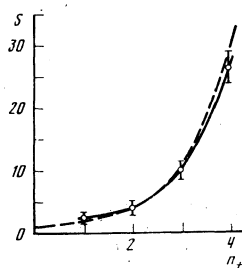


FIG. 11. Sodium-atom detection selectivity as a function of the discrimination threshold at a detuning  $\Delta\nu = 0.036 \text{ cm}^{-1}$  from the center of the absorption line.



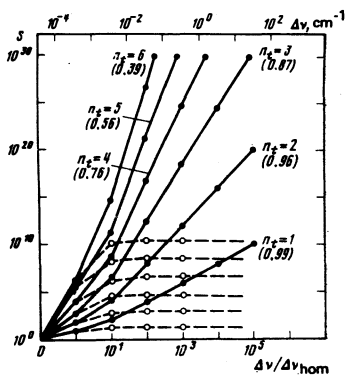


FIG. 12. Atom-detection selectivity as a function of the detuning from the absorption line center at different values of the discrimination threshold for a Lorentz contour (the quantities in the parenthesis are the probabilities of the atom registration).

concentrations  $N$  and  $n$  is the same, the detection selectivity determines the possibility of observing the smaller concentration against the background of the larger at the frequency  $\nu_L = \nu_{0n}$ ;  $\Delta\nu = \nu_{0N} - \nu_{0n}$ . The smallest observable concentration is

$$n = S_n N, \quad (15)$$

It is of interest to estimate the detection selectivity as a function of the detuning from the absorption-line center.

Figure 12 shows plots of the selectivity of atom detection against the detuning from the absorption-line center for different values of the discrimination threshold in the case of a Lorentz contour (solid curves). The plots are based on Eq. (13) for an average number  $n_0 = 5$  of the photoelectrons received from the atoms at the center of the absorption line. It is seen from the figure that for a small decrease of the registration probability of the atoms the detection selectivity can reach a value  $10^{30}$ . In a real experiment, the maximum selectivity is limited by the presence of parasitic noise.

In our experiment this noise consists of the background laser stray illumination. The minimum background signal in one channel in the experimental was  $3 \times 10^3$  pulses per second. This correspond to an average number of background photoelectrons during the registration time  $\bar{n}_0 = 4.5 \times 10^{-2}$ . This quantity determines the maximum selectivity of detection of sodium atoms in our experiment.

Figure 12 shows the calculated dependence of the detection selectivity of sodium atoms with account taken of the background stray laser illumination in our experiment (dashed line). It is seen that the

presence of the background signal limits the detection selectivity, but even in this case the detection selectivity in multiphoto electron registration of the signal is larger by many orders of magnitude that the detection selectivity of the usual registration method ( $n_t = 1$ ).

Simultaneously with the increase of the detection selectivity, the atom registration probability decreases in multiphotoelectron signal registration. For example, it is seen from Fig. 12 that the atom registration probability at the discrimination threshold  $n_t = 5$  amounts to 0.56.

In conclusion, the authors thank O. V. Terent'ev and G. I. Bekov for help with the experiment, and V. G. Minogin for numerous and helpful discussions of the results.

- <sup>1</sup>V. S. Letokhov, Usp. Fiz. Nauk **118**, 199 (1976) [Sov. Phys. Usp. **19**, 109 (1976)].
- <sup>2</sup>V. S. Letokhov, Laser Spectroscopy, Academic-Verlag, Berlin, 1977.
- <sup>3</sup>W. M. Fairbank, Jr., T. W. Hansch, and A. L. Schawlow, J. Opt. Soc. Am. **65**, 199 (1975).
- <sup>4</sup>V. I. Balykin, V. S. Letokhov, V. I. Mishin, and V. A. Semchishen, Pis'ma Zh. Eksp. Teor. Fiz. **24**, 475 (1976) [JETP Lett. **24**, 436 (1976)].
- <sup>5</sup>V. I. Balykin, V. S. Letokhov, V. I. Mishin, and V. A. Semchishen, Pis'ma Zh. Eksp. Teor. Fiz. **26**, 492 (1977) [JETP Lett. **26**, 357 (1977)].
- <sup>6</sup>V. I. Balykin, G. I. Bekov, V. S. Letokhov, and V. I. Mishin, Proc. Sixth Internat. Conf. on Atomic Physics, Riga, 1978.
- <sup>7</sup>G. W. Greenless, D. L. Clark, S. L. Kaufman, D. A. Dewis, J. F. Tonn, and J. U. Broadhurst, Opt. Commun. **23**, 236 (1977).
- <sup>8</sup>V. S. Letokhov, in: Tunable Lasers and Applications, Proc. Intern. Conf., Norway, Loen, 1976. Springer-Verlag, Berlin-Heidelberg-New York, 1976, p. 122.
- <sup>9</sup>V. S. Letokhov, in: Frontiers in Laser Spectroscopy, Proc. Les Houches Summer School, 1975, Vol. 2, North-Holland Publishing Co., 1977, p. 771.
- <sup>10</sup>A. S. Hurst, M. H. Nayfeh, and J. P. Young, Phys. Rev. B **15**, 2293 (1977).
- <sup>11</sup>G. I. Bekov, V. S. Letokhov, and V. I. Mishin, Pis'ma Zh. Eksp. Teor. Fiz. **27**, 52 (1978) [JETP Lett. **27**, 47 (1978)].
- <sup>12</sup>G. I. Bekov, V. S. Letokhov, V. I. Mishin, and O. I. Matveev, Opt. Lett. **2**, No. 3 (1978).
- <sup>13</sup>R. E. Grove, E. Y. Wu, and S. Ezekiel, Phys. Rev. B **15**, 227 (1977).
- <sup>14</sup>M. L. Citron, H. R. Gray, C. W. Gabel, and C. R. Stroud, Jr., Phys. Rev. B **16**, 1507 (1977).
- <sup>15</sup>M. Ross, Laser Receivers, Wiley, 1966.
- <sup>16</sup>D. B. Owen, Collected Statistical Tables (Russ. transl.), 1966, p. 259.
- <sup>17</sup>V. A. Karnaukhov and S. N. Polikanov, Pis'ma Zh. Eksp. Teor. Fiz. **25**, 328 (1977) [JETP Lett. **25**, 304 (1977)].

Translated by J. G. Adashko